JOURNAL OF Materials CHEMISTRY

Surface-controlled growth of magnesium oxide thin films by atomic layer epitaxy

Matti Putkonen,[a] Leena-Sisko Johansson,[b] Eero Rauhala[c] and Lauri Niinistö*[a]

[a]*Laboratory of Inorganic and Analytical Chemistry, Helsinki University of Technology, P.O. Box 6100, FIN-02150 Espoo, Finland. E-mail: Lauri.Niinisto@hut.fi*
[b]*Center of Chemical Analysis, Helsinki University of Technology, P.O Box 6100, FIN-02150 Espoo, Finland*
[c]*Accelerator Laboratory, University of Helsinki, P.O. Box 43, FIN-00014 Helsinki, Finland*

Received 28th May 1999, Accepted 13th July 1999

Magnesium oxide thin films were deposited on soda lime and Si(100) substrates by atomic layer epitaxy from $Mg(thd)_2$ and ozone. The depositions were carried out at 180–450 °C, where the growth parameters were studied in detail. A narrow temperature range of 225–250 °C was found where the growth was surface-controlled with growth rates of 0.27 and 0.22 Å cycle^{-1} on glass and silicon, respectively. MgO films were characterized by X-ray diffraction (XRD), Rutherford backscattering (RBS), X-ray photoelectron spectroscopy (XPS) and atomic force microscopy (AFM).

Introduction

Due to their thermodynamic stability and wide-bandgap insulator characteristics magnesium oxide thin films have been used as buffer layers for superconducting[1,2] and ferroelectric[3,4] materials. Also, their use as secondary emission materials for plasma display panels has recently attracted interest.[5,6]

Magnesium oxide thin films have been deposited by various different techniques. Both chemical and physical gas phase methods, as well as those employing the liquid phase (sol–gel), have been reported. Chemical methods include spray pyrolysis,[7] chemical vapor deposition (CVD)[8–12] and plasma-enhanced CVD (PECVD)[13–15] as well as liquid phase sol–gel processes.[16–18]Additionally, physical methods such as sputtering,[5,19–21] electron beam evaporation,[22–24] pulsed laser deposition (PLD),[2,4,25] laser ablation[26–28] and molecular beam epitaxy (MBE)[29] have been frequently employed.

Because no simple volatile compounds of alkaline earths exist,[30] the CVD processes have employed magnesium β-diketonates as precursors. Typically, magnesium acetylacetonate $[Mg(acac)_2]$[9,11] and magnesium 2,2,6,6-tetramethyl-3,5-heptadione $[Mg(thd)_2]$[12] have been used, but the use of true metallo-organic compounds such as cyclopentadienyl magnesium has also been reported.[31] The volatile magnesium 2-ethylhexanoate complex has also been employed.[10]

Recently Atomic Layer Epitaxy (ALE) has been succesfully applied to the growth of thin films of a number of binary oxides in a controlled manner.[32,33] Through its inherent surface control, the ALE process has some advantageous features over CVD such as conformal coating, demonstrated recently in extreme cases.[34,35] Here we report for the first time the deposition of MgO thin films by ALE using a magnesium β-diketonate and ozone as reactants.

Experimental

Thin film depositions were carried out in a flow-type hot-wall Atomic Layer Epitaxy (ALE) reactor, described in detail elsewhere.[36,37] Source materials were pulsed alternately into the reactor chamber and nitrogen (99.999%) was used as a carrier and purging gas. 5×5 cm^2 samples of soda lime and Si(100) were used as substrates. The nitrogen flow rate was 470 cm^3 min^{-1}. The source material for magnesium was $Mg(thd)_2$ (thd = 2,2,6,6-tetramethyl-3,5-heptadione), synthesised from >99% $Mg(NO_3)_2$ (Merck). $Mg(thd)_2$ was evaporated from an open aluminium crucible at 170 °C. Ozone generated from O_2 (99.999%) in an ozone generator (Fischer model 502) was used as the oxidizing reactant. The concentration of ozone was about 3.5% and no additional carrier gas was used for the O_3/O_2 mixture, which had a flow rate of 75 cm^3 min^{-1}. The total reactor pressure was 1 mbar during the deposition. The effect of the deposition temperature on the growth rate was studied over the temperature range 180–450 °C. Also, the effect of the precursor pulsing times of $Mg(thd)_2$ and O_3 (0.5–3.0 and 3.0–20.0 s, respectively) as well as that of the purging time between the reactant pulses (0.5–4.0 s) were investigated.

The volatility of the $Mg(thd)_2$ precursor and its thermal stability were checked by simultaneous TG/DTA measurements (Seiko SSC 5200) in the temperature range 20 to 400 °C. 1 mbar pressure and a small nitrogen (99.999%) flow were used to simulate the ALE deposition conditions.[38] The thicknesses of the deposited MgO thin films were measured by profilometry (Sloan Dektak 3030ST from Veeco Instruments). The steps were etched by dilute hydrochloric acid. The crystallite orientations of the MgO thin films were determined by X-ray diffraction using Cu-Kα radiation (Philips MPD 1880). Surface morphology and typical grain sizes were studied with a Nanoscope III atomic force microscope using a scanning area of 300×300 nm.

The Rutherford backscattering (RBS) experiments were performed at the University of Helsinki. The 2.0 MeV $^4He^+$ ion beam was generated by the 2.5 MV Van de Graaff accelerator of the Accelerator Laboratory. The energy calibration of the beam-analyzing magnet was based on the resonance at 1799.8 keV of the reaction $^{27}Al(p,\gamma)^{28}Si$. The scattering chamber was 0.7 m in diameter and was equipped with a Si surface barrier detector (50 mm^2, 100 μm), positioned at a scattering angle of 170°. The detector solid acceptance angle was 7.85 msr and the detector to target distance 70 mm. Standard electronics were used with the energy resolution of the detection system being 15 keV. The aperture of beam incidence, the target and the center of the detector were all placed in a horizontal plane in the chamber. During measurement, the samples were tilted with respect to a vertical axis until the beam was aligned along the (100) crystal plane of the silicon substrate. By using this arrangement the yield from

Si was significantly suppressed and the O and Mg peaks became more visible.

One sample, deposited at 250 °C over 5000 cycles, was also analysed with an XPS electron spectrometer (AXIS 165 by Kratos Analytical), using monochromated Al-Kα irradiation at 100 W. The sample was fresh but air-exposed and was measured without a further cleaning procedure or sputtering. The area of analysis was less than 1 mm^2 and the sample was analysed at three different points. The sample surface was neutralized during the data acquisition with slow thermal electrons.[39] The binding energy scale was calibrated for each measurement using the C 1s signal from C–C bonds at 285.0 eV.

Results and discussion

TG/DTA studies indicated the almost complete volatility of the $Mg(thd)_2$ precursor. The TG curve onset was at 170 °C. An endothermic DTA peak shows that $Mg(thd)_2$ melts at 128 °C, which is slightly lower than the melting point temperature obtained under atmospheric pressure.[40] Melting before volatilization ensures a more stable volatilization rate during deposition compared to solid, sublimating precursors although for ALE the precursor dose is not critical as long as there is surface saturation at the substrate. The TG data were used to select the source temperature for the precursor in the subsequent ALE depositions. The dependence of growth rate on temperature is presented in Fig. 1. The highest growth rate (0.27 Å cycle^{-1}) on soda lime glass was observed over the narrow plateau in the temperature range from 225 to 250 °C. Even there the growth rate is much less than one monolayer per cycle [0.13 monolayers cycle^{-1} in the (100) orientation], which is due to the steric hindrance of the bulky $Mg(thd)_2$ molecule, leading to a partial surface coverage. Another growth mechanism with a lower growth rate is dominant in the temperature range 300–350 °C. This is probably due to decomposition of the $Mg(thd)_2$ species in the gas phase. Finally, a slight increase in growth rate was observed at the temperature range 350 to 450 °C, which was probably due to gas phase reactions near the surface leading to uncontrolled growth at an enhanced rate.

Typical ALE-type growth below 250 °C was verified by studying reactant pulse and purge times at 250 °C. The growth rate of MgO thin films was dependent on both reactants at shorter pulsing times. Surface saturation during the $Mg(thd)_2$ pulse was obtained with pulse times over 1.0 s after which the growth rate remained constant (Fig. 2). A slightly lower growth rate (0.22 Å cycle^{-1}) was observed on (100) silicon, although the orientation remained the same.

Ozone pulses significantly longer than 1 s were needed to obtain MgO thin films. A complete reaction was obtained only after a 5.0 s O_3 pulse and increasing the pulse times to 20 s brought about no increase in the growth rate, indicating that

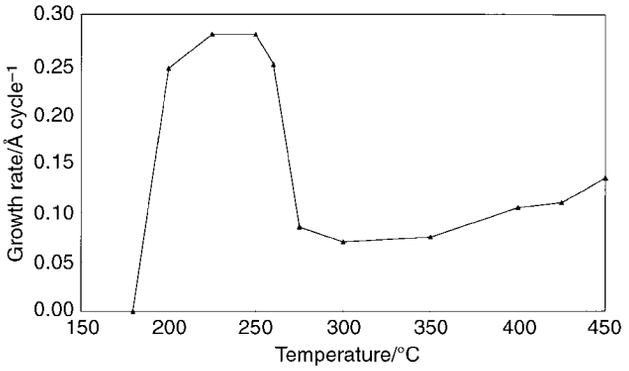

Fig. 1 Deposition rate of magnesium oxide thin film as a function of reactor temperature.

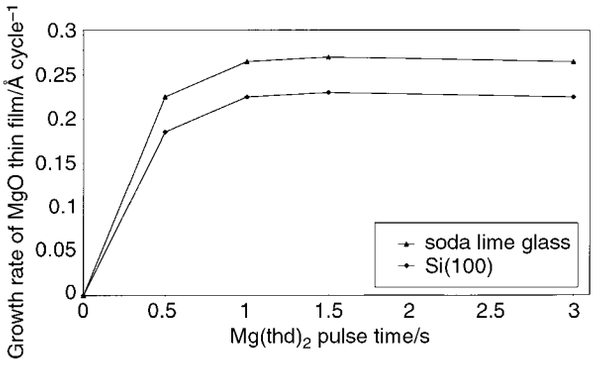

Fig. 2 Deposition rate as a function of $Mg(thd)_2$ pulse time. Source and reactor temperatures are 170 and 250 °C, respectively. O_3 pulse time 5.0 s.

only a surface-controlled reaction was occurring. Such a long O_3 pulse time indicates low reactivity between $Mg(thd)_2$ and ozone at 250 °C. When the reactant pulses were separated by a 1.5 s nitrogen purge, a constant growth rate was obtained.

The dependence of the MgO thin film thickness on the number of reaction cycles at 250 °C is presented in Fig. 3. Depositions carried out in the ALE window resulted in a linear dependency of the film thickness on the number of cycles carried out.

Throughout the temperature range studied, from 200 to 450 °C, only the (200) peak of periclase MgO was detected when deposition was carried out over 3000 cycles or less, resulting in a MgO thin film thickness below 80 nm on soda lime glass or below 66 nm on (100) silicon. When 5000 cycles were used at 250 °C [film thickness 135 nm on soda lime glass and 110 nm on (100) silicon], the (220) peak was also observed regardless of the substrate (Fig. 4). When deposition was carried out under optimised conditions at 250 °C, thickness

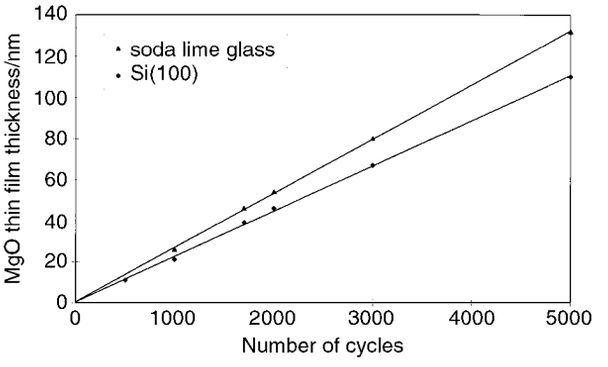

Fig. 3 Thickness dependence of magnesium oxide thin films as a function of number of deposition cycles. Source and reactor temperatures are 170 and 250 °C, respectively. $Mg(thd)_2$ and O_3 pulse times are 1.5 and 5.0 s, respectively.

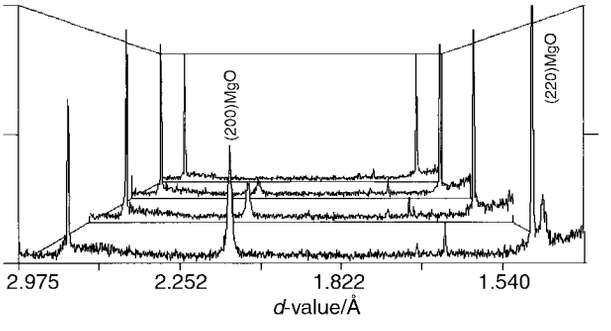

Fig. 4 XRD patterns of MgO films deposited at 250 °C on (100) silicon after different numbers of cycles. From top to bottom; 500, 1700, 2000 and 5000 cycles. Unidentified peaks are from the silicon substrate.

variations were very small ($\pm 1\%$) within the substrate length of 5 cm. No signs of spinel-like MgO were seen in the XRD patterns of films deposited onto silicon, but here the substrate had a different orientation (100) than that (111) used by Menon and Bullard.[18]

AFM images were taken from MgO thin films deposited at 250 °C onto soda lime glass. Images were collected from MgO thin film samples whose thicknesses varied from 15 to 135 nm, predetermined by the number of ALE reaction cycles. No major differences in the grain size were observed when the number of reaction cycles was varied from 500 to 5000 [Fig. 5(a–c)]. This is probably an indication that columnar growth dominates after the grain size has reached *ca.* 30 nm. The roughness (rms) of the deposited MgO thin films increased as a function of thickness from 0.51 to 1.33 nm (Table 1).

During the second stage of AFM analysis, a comparison was made between MgO thin films deposited onto soda lime glass and (100) silicon. The grain sizes were *ca.* 30 nm on both substrates indicating similar growth mechanism [Fig. 5(c,d)]. Slightly larger grains and a smoother surface were observed on a MgO thin film deposited on (100) silicon. Roughness values (rms) were of the same order of magnitude, *viz.* 1.33 nm on soda lime glass and 1.02 nm on (100) silicon for MgO films deposited over 5000 cycles.

MgO stoichiometry was measured from a sample deposited at 250 °C using optimized parameters. The RBS spectra were taken with a beam of 2.0 MeV $^4He^+$ ions. By way of an example, a representative spectrum is depicted in Fig. 6, together with the calculated oxygen and magnesium peaks shown on the yield from the silicon substrate. The silicon yield was reduced due to channeling along the (100) crystal plane. The solid curve connecting the experimental data points and the elemental O and Mg signals is a result of a computer fit,[41] which was obtained by successively calculating theoretical computer simulated spectra, varying the composition and areal density of the MgO film until a good match between the experimental and theoretical spectra was obtained. An atomic ratio of 1.05 ± 0.10 for Mg and O and an areal density of $890 \pm 20 \times 10^{15}$ atoms cm^{-2} resulted for the film depicted in Fig. 6.

Table 1 Roughness as a function of MgO thin film thickness on soda lime glass

Thickness/nm	Number of cycles	Roughness (rms)/nm
14	500	0.51
45	1700	0.65
135	5000	1.33

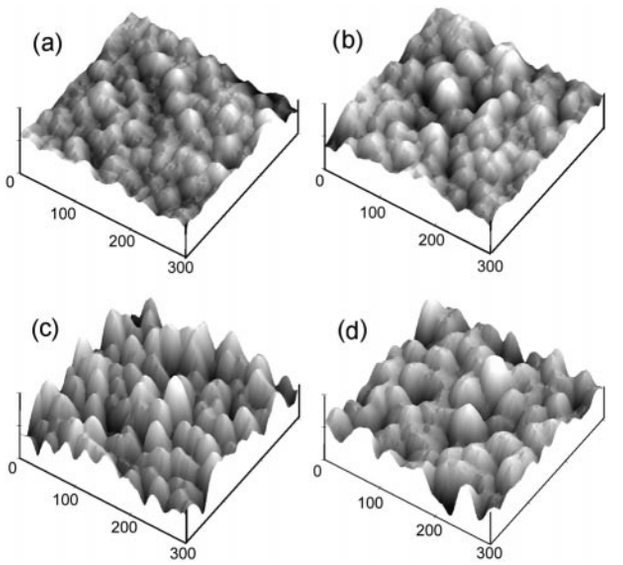

Fig. 5 MgO thin film surface morphology as a function of thickness measured by AFM from a 300×300 nm area, height axis 5 nm; (a) 15, (b) 45, (c) 135, (d) 110 nm. Soda lime (a–c) and Si(100) substrates (d) were employed.

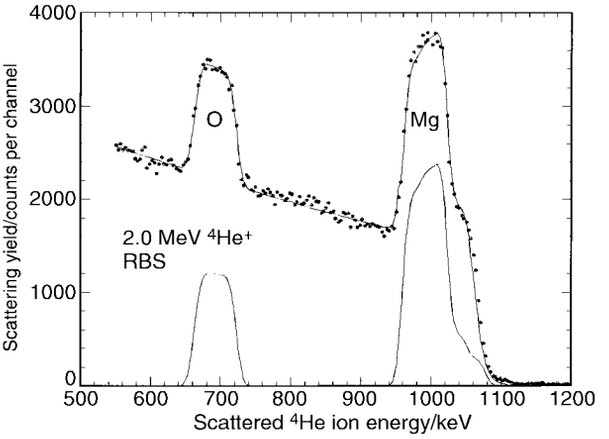

Fig. 6 A Rutherford backscattering spectrum for 2.0 MeV $^4He^+$ ions incident on a magnesium oxide film on a silicon substrate. The points denote the experimental spectrum, the solid line connecting the points is a computer simulation. The computer calculated elemental signals of O and Mg are also shown. The scattering angle is 170° and channel width 3 keV.

According to the survey spectra (0–1100 eV) of the XPS analysis, the MgO film surface consisted of oxygen, magnesium, carbon and small amounts of sodium (1.1–1.5 at.%) [Fig. 7(a)]. The carbon C 1s signal consisted mainly of C–C bonds, typical of surface contamination; small amounts of C–O and O–C=O bonds were also detected.[42] For the chemical identification of surface species, high resolution spectra of the O 1s and Mg 2p regions were recorded using a 20 eV analyser pass energy and 0.1 eV steps [Fig. 7(b) and (c)]. The binding energy of the Mg 2p signal at 50.1 eV was in good agreement with the tabulated values for MgO.[42,43] The oxygen O 1s signal could be resolved into two roughly equal components. The

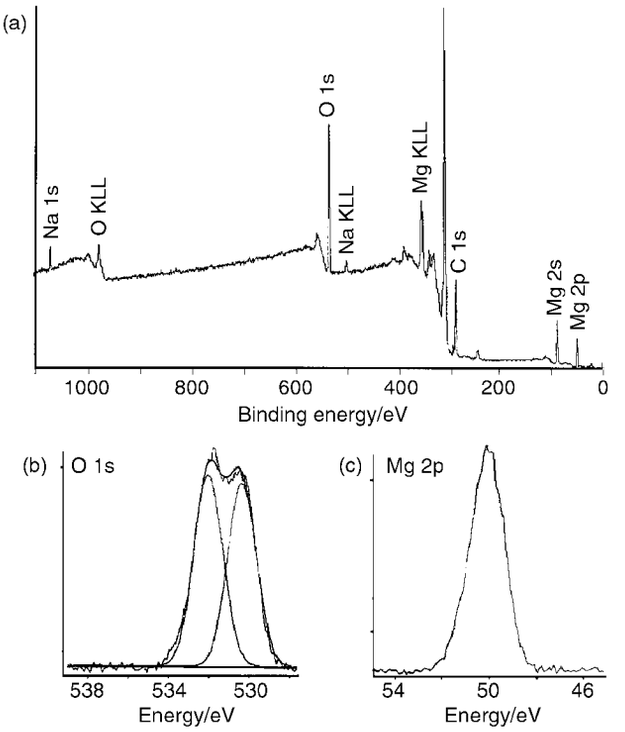

Fig. 7 XPS wide binding energy spectrum of MgO deposited at 250 °C (a) and XPS high resolution spectra of O 1s (b) and Mg 2p (c) regions.

binding energy of the low energy component at 530.4 eV was in accordance with the tabulated values for MgO.[42,43] The other component at 532.2 eV was identified as due to a hydroxide species, which are expected to cover the hygroscopic MgO surface, even after brief exposures to the atmosphere. The atomic ratio of $Mg:O_{MgO}$ species was stoichiometric, *i.e.* 1 : 1. The binding energies of the MgO species were in good agreement with the measurements performed by us for other MgO materials.[44]

Conclusions

MgO thin films can be deposited by atomic layer epitaxy using a volatile β-diketonate complex of magnesium [$Mg(thd)_2$] and ozone as precursors. A narrow temperature range of 225–250 °C was found where the growth was surface-controlled. After optimisation of Mg precursor and purge gas times, homogenous depositions over the 5×5 cm^2 substrate area were observed with thickness variations of only $\pm 1\%$. Due to the bulky Mg precursor and its limited reactivity, the growth rate at 250 °C remained low, being 0.27 and 0.22 Å cycle^{-1} on soda lime and Si(100), respectively. The relationship between the number of cycles and the thickness of the deposited film was perfectly linear throughout the range studied.

The MgO films were polycrystalline (periclase-type) exhibiting only the (200) peak for thinner films. An additional peak (220) appeared for samples deposited over 500 cycles or more, corresponding to 135 and 110 nm thicknesses for soda lime glass and silicon substrates, respectively. The correct MgO stoichiometry was also confirmed by both XPS and RBS measurements. According to AFM measurements, the films had a similar type of morphology regardless of the substrate and a low roughness as indicated by the rms values of around 1 nm.

The present study demonstrates for the first time that ALE can also be used to deposit MgO. The resulting films on soda lime and silicon substrates are polycrystalline and homogenous showing a preferred (200) orientation as thin layers and a very small thickness variation. Because the growth rate is rather low, the ALE process cannot compete with the sol–gel method, for instance. However, the film quality, together with the possibility of having a perfect conformal coating, makes ALE an attractive alternative for special applications.

Acknowledgement

The authors wish to thank Mr Mikko Utriainen, Lic. Techn., for the AFM measurements.

References

1 S. Nagaoka, K. Hamasaki, T. Yamashita and T. Komata, *Jpn. J. Appl. Phys.*, 1989, **28**, 1367.
2 D. K. Fork, F. A. Ponce, J. C. Tramontana and T. H. Geballe, *Appl. Phys. Lett.*, 1991, **58**, 2294.
3 A. N. Basit, H. K. Kim and J. Blachere, *Appl. Phys. Lett.*, 1998, **73**, 3941.
4 K. Nashimoto, D. K. Fork and T. H. Geballe, *Appl. Phys. Lett.*, 1992, **60**, 1199.
5 K. Irie, S. Ishibashi, T. Nishimura, H. Fujii, S. Muraji, Y. Shima and H. Hasuyama, *Key Eng. Mater.*, 1999, **159–160**, 299.
6 E.-H. Choi, H.-J. Oh, Y.-G. Kim, J.-J. Ko, J.-Y. Lim, J.-G. Kim, D.-I. Kim, G. Cho and S.-O. Kang, *Jpn. J. Appl. Phys.*, 1998, **37**, 7015.
7 O. Strycmans, T. Segato and P. H. Duvigneaud, *Thin Solid Films*, 1996, **283**, 17.
8 J.-H. Boo, K.-S. Yu, W. Koh and Y. Kim, *Mater. Lett.*, 1996, **26**, 233.
9 K. Kamata, Y. Shibata and Y. Kishi, *J. Mater. Sci. Lett.*, 1984, **3**, 423.
10 T. Maruyama and J. Shianoya, *Jpn. J. Appl. Phys.*, 1990, **29**, L810.
11 J. M. Zeng, H. Wang, S. X. Shang, Z. Wang and M. Wang, *J. Cryst. Growth*, 1996, **169**, 474.
12 B. S. Kwak, E. P. Boyd, K. Zhang, A. Erbil and B. Wilkins, *Appl. Phys. Lett.*, 1989, **54**, 2542.
13 E. Fujii, A. Tomozawa, S. Fujii, H. Torii and R. Takayama, *Jpn. J. Appl. Phys.*, 1994, **33**, 6331.
14 Y.-W. Zhao and H. Suhr, *Appl. Phys. A*, 1992, **54**, 451.
15 E. Fujii, A. Tomozawa, S. Fujii, H. Torii, M. Hattori and R. Takayama, *Jpn. J. Appl. Phys.*, 1993, **73**, L1448.
16 A. A. Rywak, J. M. Burlitch and T. M. Loehr, *Chem. Mater.*, 1995, **7**, 2028.
17 J.-G. Yoon and K. Kim, *Appl. Phys. Lett.*, 1995, **66**, 2661.
18 M. Menon and J. W. Bullard, *J. Mater. Chem.*, 1999, **9**, 949.
19 W.-Y. Hsu and R. Raj, *Appl. Phys. Lett.*, 1992, **60**, 3105.
20 Y. Hakuraku, K. Maezono and H. Ueda, *Supercond. Sci. Technol.*, 1996, **9**, 775.
21 Y. Kaneko, N. Mikoshiba and T. Yamashita, *Jpn. J. Appl. Phys.*, 1995, **30**, 1091.
22 L. S. Hung, L. R. Zheng and T. N. Blanton, *Appl. Phys. Lett.*, 1992, **60**, 3129.
23 H. Z. Durusoy, *J. Mater. Sci. Lett.*, 1991, **10**, 1023.
24 L. D. Chang, M. Z. Tseng, E. L. Hu and D. K. Fork, *Appl. Phys. Lett.*, 1992, **60**, 1753.
25 E. J. Tarsa, M. De Graef, D. R. Clarke, A. C. Gossard and J. S. Speck, *J. Appl. Phys.*, 1993, **73**, 3276.
26 P. A. Stampe and R. J. Kennedy, *J. Cryst. Growth*, 1998, **191**, 472.
27 P. A. Stampe and R. J. Kennedy, *J. Cryst. Growth*, 1998, **191**, 478.
28 P. A. Stampe and R. J. Kennedy, *Thin Solid Films*, 1998, **326**, 63.
29 S. Yadavalli, M. H. Yang and C. P. Flynn, *Phys. Rev. B*, 1990, **41**, 7961.
30 M. Tiitta and L. Niinistö, *Chem. Vap. Deposit.*, 1997, **3**, 167.
31 R. Huang and A. H. Kitai, *Appl. Phys. Lett.*, 1992, **61**, 1450.
32 L. Niinistö, M. Ritala and M. Leskelä, *Mater. Sci. Eng., B*, 1996, **41**, 23.
33 L. Niinistö, *Curr. Opin. Solid State Mater. Sci.*, 1998, **3**, 147.
34 C. Dücsö, N. Q. Khanh, Z. Horváth, I. Barsony, M. Utriainen, S. Lehto, M. Nieminen and L. Niinistö, *J. Electrochem. Soc.*, 1996, **143**, 683.
35 M. Ritala, M. Leskelä, J.-P. Dekker, C. Mutsaers, P. J. Soininen and J. Skarp, *Chem. Vap. Deposit.*, 1999, **5**, 7.
36 T. Suntola, A. Pakkala and S. Lindfors, *US Pat.* 4413033, 1983.
37 M. Leskelä and L. Niinistö, in *Atomic Layer Epitaxy*, ed. T. Suntola and M. Simpson, Blackie, Glasgow, 1990, p. 3.
38 M. Leskelä, L. Niinistö, E. Nykänen, P. Soininen and M. Tiitta, *Thermochim. Acta*, 1995, **175**, 91.
39 *Axis 165 Operating Manual and User's Guide*, Kratos Analytical Ltd, Manchester, 1995.
40 K. J. Eisentraut and R. E. Sievers, *J. Am. Chem. Soc.*, 1965, **87**, 5254.
41 J. Saarilahti and E. Rauhala, *Nucl. Instrum. Methods Phys. Res., Sect. B*, 1992, **64**, 734.
42 *Handbook of X-Ray Photoelectron Spectroscopy*, ed. J. Chastain and R. C. King, Jr., Physical Electronics, Eden Prairie, 1995, p. 41.
43 S. Ardizzone, C. L. Bianchi, M. Fadoni and B. Vercelli, *Appl. Surf. Sci.*, 1997, **119**, 253.
44 M. Putkonen and L.-S. Johansson, unpublished results.

Paper 9/04315B